DOI: 10.61782/fa.2025.0724

FORUM ACUSTICUM EURONOISE 2025

RAINBOW TRAPPING RESONATOR ARRAY FOR HIGH-LEVEL SOUND ABSORPTION

Adam Cavanagh[1*] **Olga Umnova**[1] **Deepak Akiwate**[1]
[1] University of Salford, Acoustics Research Centre, M5 4WT, Salford, UK

ABSTRACT

This study analyses a proof-of-concept ducted rainbow-trapping resonator array designed for high-level sound absorption. By tuning the dimensions of the array's resonators, it absorbs sound waves over a broad frequency range and with increasing efficiency with incident pressure amplitude. The arrays' acoustic behaviour was modelled numerically, where the greatest attenuation was observed at the highest level considered, 155 dB. The results show the potential applicability of absorber designs that exhibit rainbow-trapping behaviour to high-intensity environments.

Keywords: *high-amplitude sound, acoustic rainbow-trapping, resonator array, sound attenuation, resonator nonlinearity*

1. INTRODUCTION

Sound absorbers based on resonant cavities, i.e. those in perforated liners, can exhibit significant local nonlinear effects at high SPLs, impairing or enhancing absorption properties [1, 2]. The dominating nonlinear effect in resonant absorbers is the increased resistance with incident wave amplitude. A HR side-loaded to a principal waveguide can exhibit increased energy dissipation by converting the incident wave's energy to vortical kinetic energy at the sharp edges of the resonator's neck, i.e., at discontinuities. For instance, this increased dissipation can induce coherent perfect absorption at high SPLs [3]. The perforations in a liner's face sheet exhibit similar effects at high SPL. These effects have been extensively studied (see,e.g. [4, 5], and can significantly alter an absorber's intended performance.

Another approach to increase absorption is absorbers with graded spatial properties, i.e., "rainbow-trapping" structures. These are designed using arrays of critically coupled resonators with frequency-cascaded band gaps to target a broadband frequency range. This way the spatial grading results in a "slow sound" phenomenon where different frequency waves become confined to specific points along the array's length, resulting in highly efficient and even perfect absorption in transmission problems [6]. Moreover, [7] have studied in detail the acoustic properties of an acoustic black hole absorber, providing valuable insights into the effect of geometry on performance and behaviour.

Maintaining efficient broadband absorption at high SPLs remains challenging due to resonators' nonlinear effects at such levels. The works of [6, 7] highlight the effectiveness of spatially graded absorbers for broadband sound absorption, and those of [3–5] offer insights into the theory and design principles of effective high-level absorption. Together, these contributions provide a compelling foundation for designing superior broadband sound absorbers for high-intensity environments.

This work evaluates the sound absorption performance of rainbow-trapping resonator arrays (RTRAs) in linear and nonlinear acoustic regimes. Two designs are considered, the first optimised for maximum linear regime absorption and the second for maximum nonlinear regime absorption. These are respectively denoted $RTRA_1$ and $RTRA_2$ hereinafter. Notably that the present configurations and simulations are for the two-dimensional case and serve as a proof of concept for nonlinear-aware optimisation applied to rainbow-trapping absorbers. The geo-

*Corresponding author: a.a.cavanagh1@salford.ac.uk.

metric configurations and modelling approach, results and discussion, and conclusions and further work are respectively presented in 2, 3, and 4.

2. METHODOLOGY

Both structures comprise an array of $N_1 = 8$ and $N_2 = 5$ differing HRs, respectively, each side-loaded to a principal waveguide of constant height arbitrarily set to 29 mm, see Fig. 1. The RTRAs' lengths and heights are constrained to a maximum length $L_t = 100$ mm and height $H_t = 30$ mm to ensure compactness and applicability to small ducts. Four parameters describe each HR's geometric configuration due to the two-dimensional setup. These parameters are the neck and cavity lengths and widths, respectively denoted $l_n^{[n]}$, $l_c^{[n]}$, $d_n^{[n]}$, and $d_c^{[n]}$ (superscript $[n]$ denotes the n^{th} HR). Each HR is designed such that its resonance frequency f_r is close to the n^{th} value in a set $\mathcal{F}$ of N_n equally spaced frequencies over the range $f_1 = 1$ kHz to $f_N = 2$ kHz. In this way, the resonances overlap to cover a broadband frequency range due to their moderate Q factors.

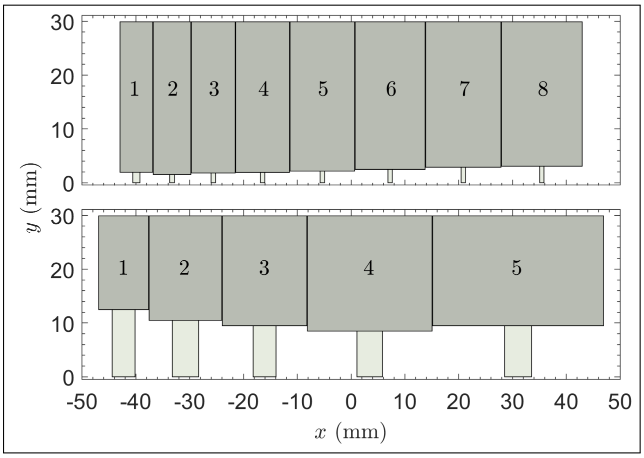

Figure 1. Linear (top) and nonlinear (bottom) optimised RTRA geometric configurations; principal waveguide is not illustrated for clarity, but is placed horizontally at $x = 0$. Geometry is in two-dimensions, meaning the structures extend infinitely into and out of the page.

2.1 Optimisation Scheme

The design process began with the development and numerical validation of an analytical model using the transfer matrix method (TMM) with effective complex and frequency-dependent density and compressibility obtained using the Johnson-Champoux-Allard equivalent fluid model [8, 9]. Then, an optimisation scheme similar to that in [6] was implemented to fine-tune the HRs dimensions. The scheme's genetic algorithm (GA) sought to minimise the cost function,

$$\mathcal{C} = \sum_{f \in \mathcal{F}} |R(f)|^2 + |T(f)|^2 + \varepsilon \,, \qquad (1)$$

i.e., to minimise the system's leakage. The quantity ε denotes a conditional penalty applied if the RTRAs' length, L, exceeds L_t ($\varepsilon = |L - L_t|$), $\varepsilon = 0$ otherwise. It controlled $l_n^{[n]}$, $d_n^{[n]}$, and $d_c^{[n]}$ with 0.01 mm minimum step size, the remaining $l_c^{[n]}$ was implicitly defined in the cost function such that $l_c^{[n]} = Ht - l_n^{[n]} - h$, where $h = 0.1$mm is a realistically manufacturable wall thickness value.

2.2 Numerical Model

Nonlinear behaviour was approximated numerically using FEM in COMSOL Multiphysics 6.2™. More precisely, nonlinear effects were accounted for using the interior perforated plate boundary condition (BC) in the Frequency Domain Pressure Acoustics interface. The BC implements the model in [4] for circular micro- and macro-perforations. Although the present configurations are in two dimensions, meaning they have slit-shaped necks, this formulation is considered acceptable under this work's conceptual nature because the underlying theory is general and applies to realistic geometries. Furthermore, the TMM's equivalent fluid model does not account for the distinct flow behaviour in larger holes and hence will not agree with FEM results for the second design, RTRA$_2$, where the neck widths are not much less than the target wavelength (see Tab. 2). While the RTRA$_1$ neck widths are significantly smaller, the TMM results were used solely for optimisation and are omitted from this work.

2.3 RTRA$_1$ – Optimised for Linear Regime

RTRA$_1$, with $N_1 = 8$ HRs side-loaded to the principal waveguide (see Fig. 1), is optimised for maximum absorption in the linear regime. The resonator geometric parameters were constrained during the optimisation process to ensure correct cascading of resonance bandgaps. See Tab. 1 for the resulting RTRA_1 resonator dimensions.

Table 1. Geometric parameters for RTRA_1. All dimensions are given in millimetres.

n	$l_n^{[n]}$	$d_n^{[n]}$	$l_c^{[n]}$	$d_c^{[n]}$
1	1.96	1.33	27.94	6.08
2	1.53	0.90	28.37	6.99
3	1.82	0.83	28.08	8.14
4	1.94	0.80	27.96	10.00
5	2.18	0.83	27.72	12.00
6	2.50	0.81	27.40	13.00
7	2.90	0.81	27.00	14.00
8	3.09	0.79	26.81	15.00

2.4 RTRA_2 – Optimised for Nonlinear Regime

RTRA_2 is designed with high SPL absorption in mind. Sound levels inside, e.g. an aeroengine can breach the nonlinear regime during flight conditions (> 150 dB) [10]. Shock waves can form at such levels if the wave can propagate sufficiently far uninterrupted. The distance a shock wave will from its sound source, known as the shock formation distance, is given by [11],

$$\overline{x} = \frac{\rho_0 c_0^3}{\omega \beta p_0'}, \tag{2}$$

where ρ_0, c_0, ω, β, and p_0' denote the density of air in kg/m^3, sound speed in air in m/s, angular frequency in rad/s, coefficient of nonlinearity in air (dimensionless) equally approximately 1.2 , and the incident wave's amplitude in Pa, respectively. Shock formation distance is inversely related to f and p_0', meaning reduction in $\overline{x}$ with increased f or p_0'. The RTRA_2's L should remain minimum one magnitude smaller than $\overline{x}$ to suppress internal shock formation.

The design accounts for nonlinear effects like flow separation and vortex shedding in the necks. These effects are realised as the dependency of the neck's acoustic resistance on incident wave amplitude, increasing the conversion of the incident wave's energy into thermal and vortical kinetic energy. Typical micro-perforation sizes present flow resistivity values that are too high for the effective transfer of wave energy into the resonators due to the non-negligible inertial effects at high SPLs. HR neck widths in RTRA_2 were thus constrained to a minimum size of 4 mm during optimisation. In this way, the GA tuned the resonators close to their respective $f \in \mathcal{F}$ while ensuring sufficiently low flow resistivity. RTRA_2 optimised dimensions are tabulated in Tab. 2.

Table 2. Geometric parameters for RTRA_2. All dimensions are given in millimetres.

n	$l_n^{[n]}$	$d_n^{[n]}$	$l_c^{[n]}$	$d_c^{[n]}$
1	12.50	4.25	17.40	9.28
2	10.50	4.89	19.40	13.51
3	9.50	4.25	20.40	15.71
4	8.50	4.75	21.40	23.18
5	9.50	5.00	20.40	31.77

3. RESULTS

Both RTRAs' performance is analysed numerically at three increasing excitation levels (80, 130, and 155 dB) to understand linear and nonlinear regime behaviour.

3.1 Linear Regime Performance

Individual resonator α is illustrated in Fig. 2. The f_r cascade is clear for both RTRAs. RTRA_1's resonators (Fig. 2 [a]) exhibit α peaks approximately over the range 750 Hz to 1720 Hz, with a gradual reduction in f from the first to last HR. Although the n^{th} HR's f_r should approximately match the corresponding $f \in \mathcal{F}$, the first four HRs exhibit maxima below 1000 Hz. This discrepancy is not too problematic (see succeeding results) and is likely attributed to the optimisation process, where the GA does not strictly know to tune each HR to each f. Conversely, most of RTRA_2's HRs present α maxima inside the target range $\mathcal{F}$, excluding the final $n = N_2$ HR.

The frequency cascade effect becomes clear when comparing the individual resonator α peaks with the full RTRA α shown in Fig. 3 (a). RTRA_1 exhibits good broadband absorption across most of the target range. The best performance is between approximately 1000–1400 Hz, with consistent $\alpha \approx 0.9$ and minimal R and T. RTRA_2 shows adequate broadband α in the linear regime despite

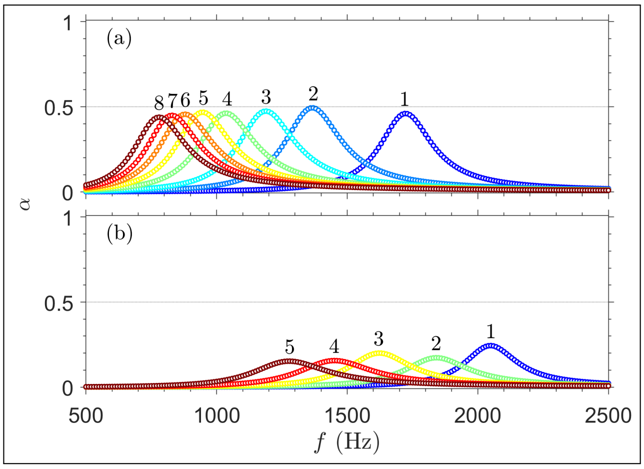

Figure 2. Sound absorption coefficients of each of the $N_1 = 8$ HRs in RTRA$_1$ (a), and for each of the $N_2 = 5$ HRs in RTRA$_2$ (b). The n^{th} HR's absorption curve is indicated by the numbers located at each of the maxima. Dotted horizontal line represents maximum possible α of a single side-loaded HR, i.e., coeherent perfect absorption.

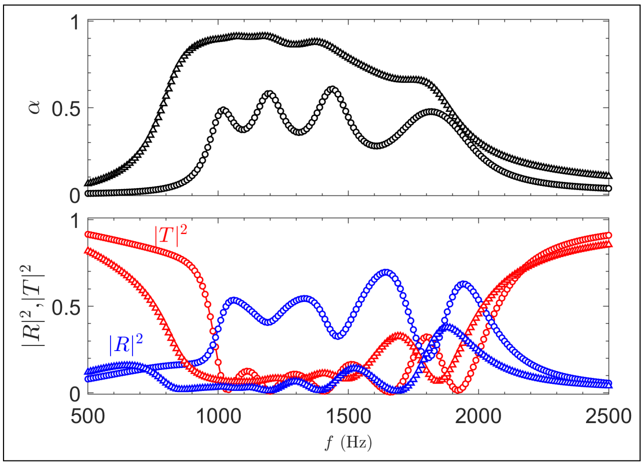

Figure 3. Sound absorption (top), reflection and transmission (bottom) coefficients obtained numerically with FEM model with 80 dB incident SPL. The coefficients for RTRA$_1$ and RTRA$_2$ are indicated by the triangle and circle markers. Red and blue curves represent reflection and transmission coefficients.

the geometric constraints. The four α peaks at approximately 1000, 1200, 1450, and 1820 Hz show the frequency cascade effect clearly, where the n^{th} and $n^{th} + 1$ HR resonances accumulate [1], causing maxima between their individual resonances.

3.2 Nonlinear Regime Performance

Nonlinear regime α performance for both RTRAs is presented in Fig. 4. RTRA$_1$ (Fig. 4 [a]) shows a pronounced deterioration from the broadband $\alpha \approx 0.85$ at 80 dB to a broadband $\alpha \approx 0.75$ at 155 dB. This behaviour is mainly due to the neck's small widths, which increases flow resistivity at higher SPLs (i.e., reduced wall admittance in the neck). Notably, the first resonator ($f_r \approx 1720$ Hz) shows an increased α at 130 dB, which then deteriorates at 155 dB. This behaviour can be attributed mostly to the relatively large d_n^1 chosen by the GA, the perforation size is large enough to increase dissipation in the weakly nonlinear regime, but is too small to behave in the same way in the full nonlinear regime.

RTRA$_2$ (Fig. 4 [b]) exhibits significant α growth with incident SPL. The necks' larger widths (see Tab. 2) performed as intended and resulted in their flow resistivities having a weaker amplitude-dependency, resulting in increased dissipation and absorption as expected.

4. CONCLUSIONS AND FURTHER WORK

This work investigated the design and optimisation of a conceptual rainbow-trapping resonator array for high-level sound absorption. The arrays' performance were analysed numerically. Results show that, depending on the intended usage, the absorbers are effective broadband sound absorbers in both linear and nonlinear acoustic regimes. The frequency-cascaded resonances of the arrays' resonators cause efficient targetted absorption of differing frequency waves along their lengths.

Further work will focus on realising a rainbow-trapping resonator array for small ducts, including realistic geometry (e.g., axial symmetry), comparisons with TMM results and experimental data.

[1] All resonances accumulate in actuality.

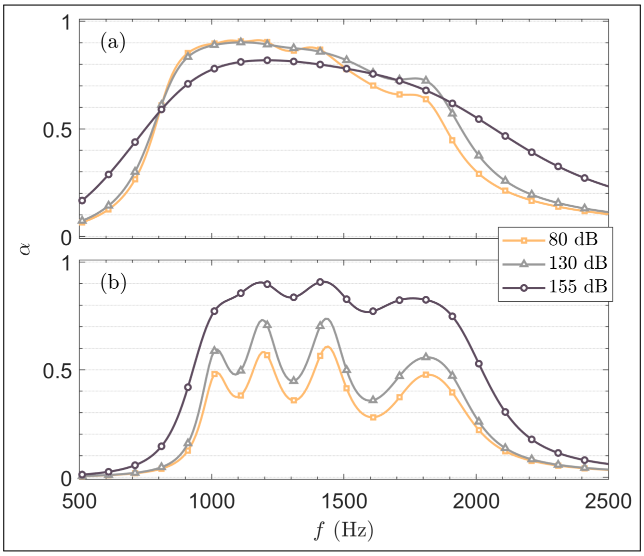

Figure 4. Sound absorption coefficients of the RTRAs at increasing incident SPLs obtained numerically with FEM model. (a) RTRA_1 (b) RTRA_2.

5. REFERENCES

[1] D. C. Brooke, O. Umnova, P. Leclaire, and T. Dupont, "Acoustic metamaterial for low frequency sound absorption in linear and nonlinear regimes," *Journal of Sound and Vibration*, vol. 485, 10 2020.

[2] M. Meissner, "The influence of acoustic nonlinearity on absorption properties of helmholtz resonators. part 1. theory," *Archives of Acoustics*, vol. 24, no. 2, pp. 179–190, 1999.

[3] V. Achilleos, O. Richoux, and G. Theocharis, "Coherent perfect absorption induced by the nonlinearity of a helmholtz resonator," *The Journal of the Acoustical Society of America*, vol. 140, pp. EL94–EL100, 07 2016.

[4] M. A. Temiz, J. Tournadre, I. L. Arteaga, and A. Hirschberg, "Non-linear acoustic transfer impedance of micro-perforated plates with circular orifices," *J. Sound Vib.*, vol. 366, pp. 418–428, 03 2016.

[5] Z. Laly, N. Atalla, and S.-A. Meslioui, "Acoustical modeling of micro-perforated panel at high sound pressure levels using equivalent fluid approach," *Journal of Sound and Vibration*, vol. 427, pp. 134–158, 08 2018.

[6] N. Jiménez, V. Romero-García, V. Pagneux, and J.-P. Groby, "Rainbow-trapping absorbers: Broadband, perfect and asymmetric sound absorption by subwavelength panels for transmission problems," *Scientific Reports*, vol. 7, 10 2017.

[7] G. Bezançon, O. Doutres, O. Umnova, P. Leclaire, and T. Dupont, "Thin metamaterial using acoustic black hole profiles for broadband sound absorption," *Applied Acoustics*, vol. 216, 01 2024.

[8] N. Jiménez, O. Umnova, and G. Jean-Philippe, eds., *Acoustic Waves in Periodic Structures, Metamaterials, and Porous Media: From Fundamentals to Industrial Applications*. Springer International Publishing, 2021.

[9] J. Allard and N. Atalla, *Propagation of sound in porous media*. Hoboken, NJ: Wiley-Blackwell, 10 2009.

[10] E. P. Ross, K. M. Figueroa-Ibrahim, S. C. Morris, D. L. Sutliff, and G. J. Bennett., "Evaluating an additive manufactured acoustic metamaterial using the advanced noise control fan," *AIAA Journal*, vol. 62, pp. 2783–2799, 07 2024.

[11] M. F. Hamilton and D. T. Blackstock, eds., *Nonlinear acoustics*. San Diego, CA: Academic Press, 11 1997.